IOP Conference Series: Earth and Environmental Science

PAPER • **OPEN ACCESS**

Dynamic Response Computation of Single-Point Mooring of Product Tanker Based on AQWA

To cite this article: Xuan Zhang *et al* 2020 *IOP Conf. Ser.: Earth Environ. Sci.* **527** 012010

Dynamic Response Computation of Single-Point Mooring of Product Tanker Based on AQWA

Xuan Zhang[1*], Jinpeng Hu[2] and Bo Hong[1]

1 Civil and Transportation College, South China University of Technology, Guangzhou, China
2 School of Port and Environmental Engineering, Jimei University, Xiamen, China
*E-mail: zx201705@outlook.com

Abstract. This paper took the product tanker at sea and its mooring positioning system as the research object and used the time-frequency domain method to calculate the movement of the product tanker. In the three-dimensional potential flow theory, a single-point mooring system was established as a numerical model in the ANSYS Workbench. The frequency-domain computing module was to analyze the hydrodynamic response of the tanker under the unit regular waves, the dynamic response amplitude operators (RAOs) of the tanker, and the motion conditions under different frequency distributions. The time-domain computing module was to analyze the response of a single-point mooring system under the actions of wind, wave, and current. Setting the mooring point, pretension, layout, mooring radius, and other parameters, of the mooring product tanker was calculated lasted 1 hour for the time-domain coupling analysis under the extreme offshore environment. The tension of each cable was compared with the minimum breaking strength of the mooring cable to determine its safety.

1. Introduction

In this paper, the three-dimensional potential flow theory is to analyze radiation and diffraction. Hence, the linear superposition theorem is to represent the velocity potential inside the fluid domain. To the mooring system, the bow cable chain is matched by polynomial nonlinear mooring catenary in AQWA, and the dynamic response of mooring catenaries is solved numerically as a discrete block-mass model. Pierson-Moskowitz spectrum is used in the time domain because it is a particular case for a fully developed long-crested sea.

Aqwa can generate a time history of the simulated motions of floating structures, arbitrarily connected by articulations or mooring lines, under the action of wind, wave, and current forces. For wind and current forces, when the surface of the marine structure is beyond average height, the wind will generate load on the hull directly. The wind force is calculated by using the wind speed at 10 m [1].

Bracco G et al. [2] focused on the implementation of a non-linear coupled model to improve the float shape to maximize the power absorption by AQWA. Buchner B et al. [3] adopted a numerical time-domain simulation model for the prediction of the hydrodynamic response of an LNG FPSO with an alongside moored LNG tanker. Huijsmans R H M et al. [4] investigated the hydrodynamical aspects of a floating two-body system. Li L et al. [5] proposed an integrated optimization method for the design of the mooring systems of a vessel-shaped offshore fish farm. Naciri M [6] used a time domain to simulate side-by-side moored vessels. Pastor J et al. [7] created a linear frequency domain model to predict the behavior of a heaving point absorber using AQWA. Wang K P et al. [8] presented a frequency domain approach to predict the coupled response of a floating wind turbine based on AQWA. Xu J et al. [9] studied the properties of a small oil tanker motion in several waves under the

six degrees of freedom of RAOs, additional parameters such as quality and radiation damping. Zhang A et al. [10] studied the motion response and tension response of a tension leg platform with different pretension and the number of tendons by AQWA software.

2. Analysis method

In this paper, the Pierson-Moskowitz spectrum was chosen as an irregular wave in a hydrodynamic response. The Pierson-Moskowitz spectrum is formulated over two parameters of the significant wave height, and the average (mean zero-crossing) wave period. The significant wave height chooses 4 m, and the zero-crossing period is 6 s as the analysis method. The form used in Aqwa is considered of more direct use than the classic form, and the form involving the peak frequency. The spectral ordinate at a frequency (in rad/s) is given by

$$S(\omega) = 4\pi^3 \frac{H_S^2}{T_Z^4} \frac{1}{\omega^5} \exp(-\frac{16\pi^3}{T_Z^4} \frac{1}{\omega^4}) \tag{1}$$

The following relationship exists between T_Z, T_1, and T_0:

$$\begin{aligned} T_0 &= 1.408 T_Z \\ T_1 &= 1.086 T_Z \end{aligned} \tag{2}$$

Where T_1 is the mean wave period, and T_0 is the peak period.
Aqwa gives the definitions of the starting and finishing frequencies of the Pierson-Moskowitz spectrum as
Starting frequency (in rad/s):

$$\omega_s = 0.58 \frac{2\pi}{T_Z} \tag{3}$$

Finishing frequency (in rad/s):

$$\omega_f = 5.1101 \frac{2\pi}{T_Z} \tag{4}$$

The wind and current loads acting on the boat are calculated using the following equations:

$$\begin{aligned} F_{xw} &= 0.5 C_{xw} \rho_w V_w^2 A_T & F_{xc} &= 0.5 C_{xc} \rho_c V_c^2 L_{BP} T \\ F_{yw} &= 0.5 C_{yw} \rho_w V_w^2 A_L & F_{yc} &= 0.5 C_{yc} \rho_c V_c^2 L_{BP} T \\ M_{xyw} &= 0.5 C_{xyw} \rho_w V_w^2 A_L L_{BP} & M_{xyc} &= 0.5 C_{xyc} \rho_c V_c^2 L_{BP}^2 T \end{aligned} \tag{5}$$

The wind and current force coefficients are adopted from *the Prediction of Wind and Current Loads on VLCCs* [11]. The wind and current force coefficients of the tanker show in figure 1.

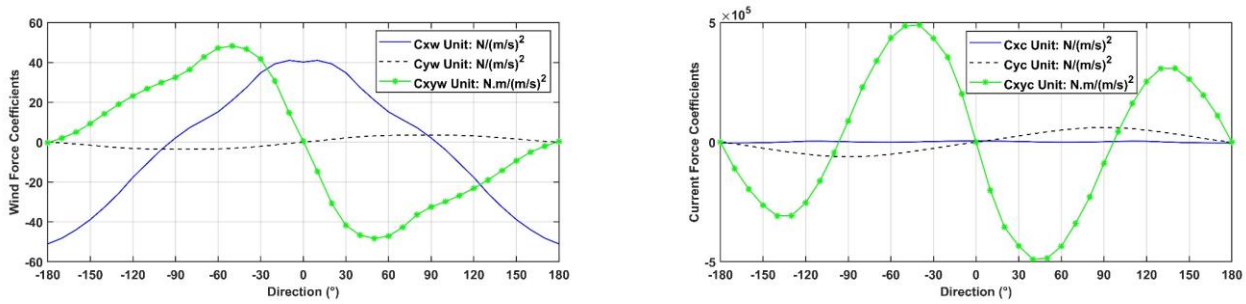

Figure 1. The wind and current force coefficients of tanker

3. Numerical simulation

3.1. The parameters of the tanker

The tanker length is 59.55 m, breadth is 10.8 m, depth is 5 m, the draught of the hull is 4 m, the simulated water depth is 21 m. The mass of the tanker is 1,000 t, the length between vertical lines is 58 m, the barycentric coordinates are (30, 0, -0.9). The transverse radius of inertia of the tanker is 3.672 m, the longitudinal radius of inertia is 15 m, the radius of inertia for rolling is 15.6 m. The lateral windward area of the tanker is 87 m^2, the vertical windward area is 8.1 m^2.

The hull has six degrees of freedom of movement, the X, Y, and Z axes represent the surge, sway, and heave, and the RX, RY, and RZ express as the roll, pitch, and yaw.

3.2. The parameters of the mooring system

The buoy is a cylinder, and its diameter is 3 m, the height is 3 m, the draught of the buoy is 2 m. The mass of the buoy is 56.38 t, the barycentric coordinates are (70, 0, -0.5). The transverse radius of inertia of the tanker is 1.061 m, the longitudinal radius of inertia is 1.061 m, the radius of inertia for rolling is 1.146 m.

There are seven cable chains in the mooring system, and the bow cable chain connects buoy with the hull, the other six connect buoy with the bottom of the sea. All the mooring chains have the same material, except for the mooring chain of a connecting tanker, the other six are of equal length and evenly distributed. The length of the bow cable chain is 9 m, other cable chains are 73 m. The mass/unit length is 200 kg/m, the equivalent cross-sectional area is 0.0169 m^2, the stiffness is 875000 kN, the maximum tension of chains is 7540 kN, the added mass coefficient is 1. The tanker and its mooring system are in figure 2. Figure 3 shows the layout of the mooring cables.

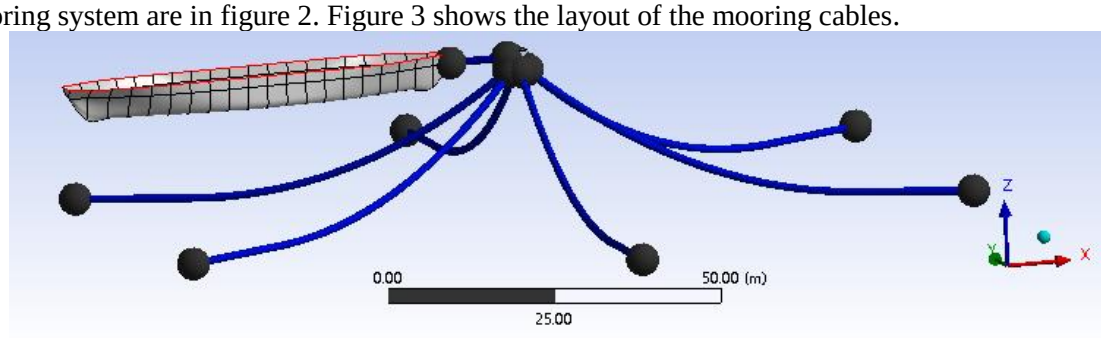

Figure 2. The product tanker and its mooring system.

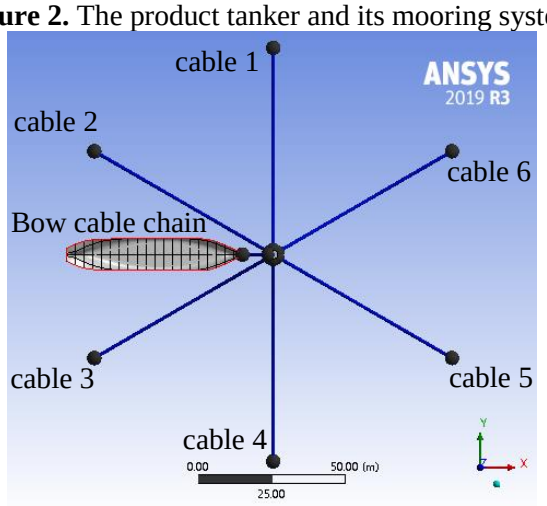

Figure 3. The layout of the mooring system.

3.3. Parameters setting

There are mesh parameters of the tanker. By choosing a combined meshing type, the defeaturing tolerance is 0.4 m, and the maximum element size is 0.8 m, the maximum allowed frequency is 0.644 Hz. The nodes are 5722, and the total elements are 5600, and diffraction nodes are 4609, and the number of diffracting elements is 4468.

After gridding and calculating the hydrodynamic diffraction, then wave parameters are required. The wave range is -180° to 180°, choosing interval is 30°, the lowest frequency is 0.01592 Hz and the highest frequency is 0.6445 Hz.
In hydrodynamic response, the Pierson-Moskowitz wave spectrum is used in numerical simulation. The average wind speed in an hour is 15 m/s, and the current speed varied with depth, the speed of the surface is 1 m/s, then gradually dropped to zero at the depth of 10 meters.
For the case 1, the direction of a wave spectrum, wind direction, and current direction is 180° respectively. In the case 2, the direction of the wave spectrum and wind direction is 180°, the current direction is 90°.

4. Results and analysis

4.1. Results of hydrodynamic diffraction

4.1.1. The added mass and radiation damping. The additional inertial force acts on the water surrounding the tanker to accelerate the water, and the water reacts to this acceleration to the tanker. Therefore, this additional inertial force is proportional to the acceleration of the tanker, and the proportionality coefficient is called the additional mass.

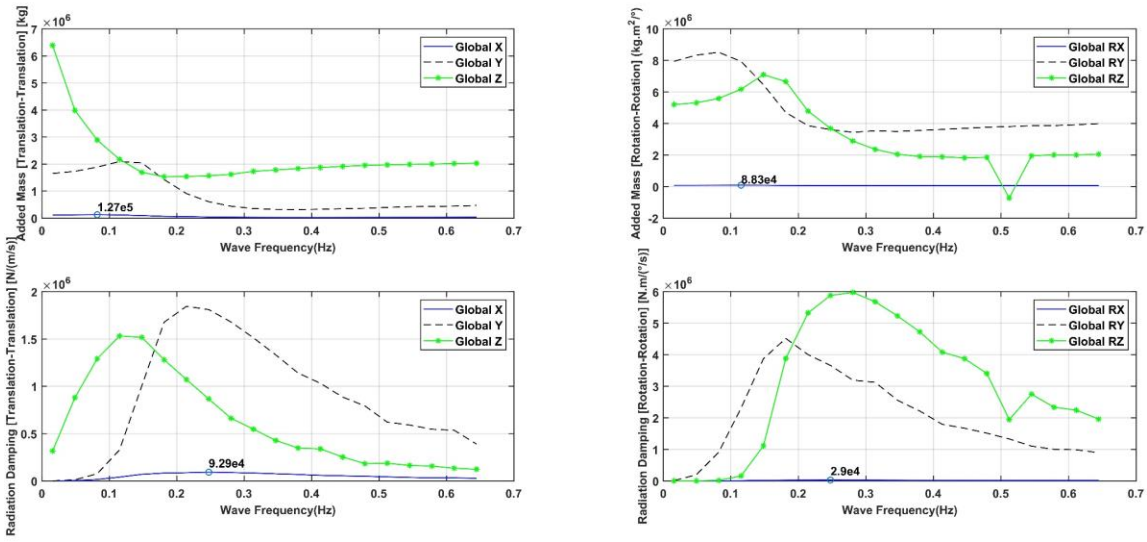

Figure 4. The added mass and radiation damping of the tanker.

As shown in figure 4, the added mess and radiation damping of surging are about one order of magnitude smaller than swaying and heaving, the added mess and radiation damping of rolling are about two orders of magnitude lower than pitching and yawing. The surging and rolling are relatively stable. The additional mass of heaving decreases with the increase of wave frequencies, and it is stable in the high-frequency region. The additional masses of surging, swaying, yawing all get the peak at the low-frequency region.
The damping coefficients of the six degrees of freedom change in a trend of increasing first and then decreasing and the maximum value appears in the frequency range of 0.15 to 0.25 Hz.

4.1.2. The results of RAOs. RAOs are usually calculated for all ship motions and all wave headings. RAOs enables to determine the amplitude of motion based on a unitary wave.
figure 5 shows the calculation results of RAOs for six degrees of freedom under four directions of wave 0°, 30°, 60°, 90°.
The RAOs of surging and swaying decreased rapidly with the increase of wave frequency, regardless of the wave directions, and values tended to 0 when the wave frequency is about 0.2 Hz. The RAOs of heaving decreased slowly with the increase of wave frequency firstly, and gradually approaches to

zero when the frequency is greater than 0.3 Hz, but the values with different wave directions varied greatly, and the peak value appeared at direction of wave 90°, which showed that the wave directions had significant impacts on the RAOs of heave.

The RAOs of rolling first increased with the increase of frequency and then decreased, there were the maximum value when the wave direction angle was 90°, and the corresponding wave frequency was 0.1813 Hz. The RAOs of the pitching and the yawing were similar, which first increased with wave frequency and then decreased. and both of pitching and yawing tended gradually to zero when the frequency is greater than 0.3 Hz.

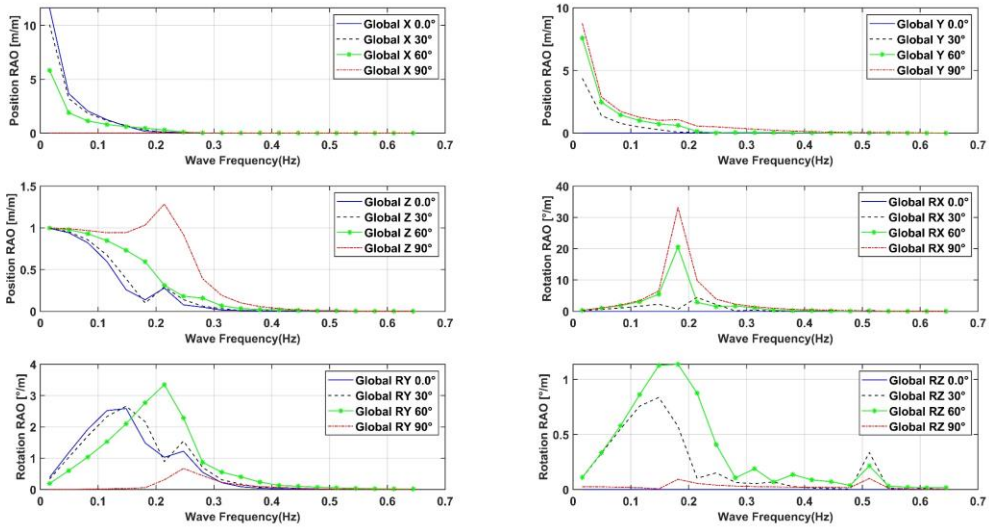

Figure 5. The amplitude response chart for six degrees of freedom under four directions of wave 0°, 30°, 60°, 90°.

4.1.3. The results of Diffraction and Froude-Krylov. In regular waves, the Froude-Krylov force makes up the total non-viscous forces with the diffraction force. Figure 6 shows the calculation results of force per unit wave amplitude for six degrees of freedom under four directions of wave 0°, 30°, 60°, 90°.

Like figure 6, the force per unit wave amplitude of surging is about one order of magnitude smaller than swaying and heaving, the moment per unit wave amplitude of rolling is about one order of magnitude smaller than pitching and yawing.

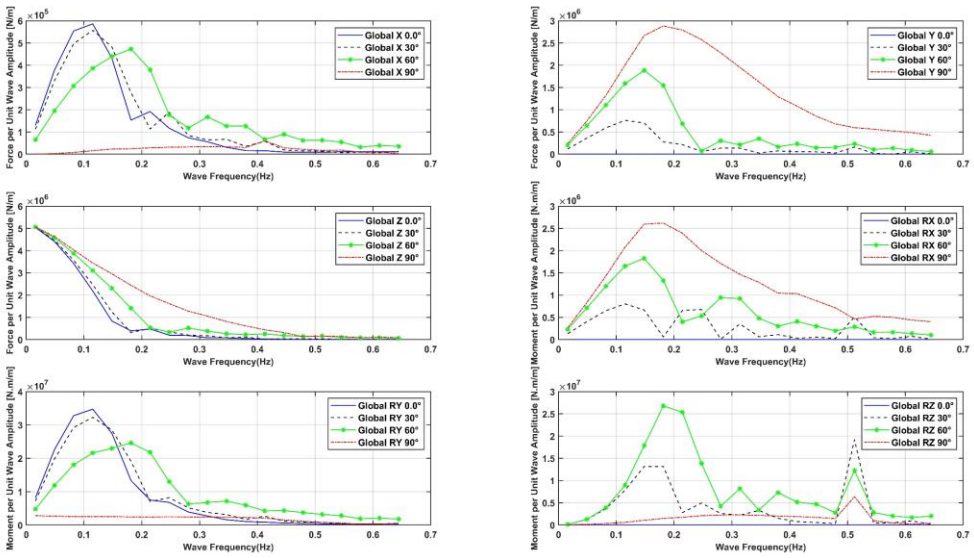

Figure 6. The force per unit wave amplitude chart for six degrees of freedom under four directions of wave 0°, 30°, 60°, 90°.

4.2. Results of hydrodynamic response

After hydrodynamic diffraction analyzing, mooring the hull with a single point mooring system. The calculation of the Hydrodynamic Response module can be used to obtain the six-degree-of-freedom motion response of the hull under different conditions over time.

In environmental conditions of the case 1, the tanker matches head against the waves, the structure positions of the hull in six degrees of freedom and the tension values of 7 mooring cables are shown in figure 7 and 8 respectively. The maximum tension of cables in the case 1 is 3811.4 kN in cable 5.

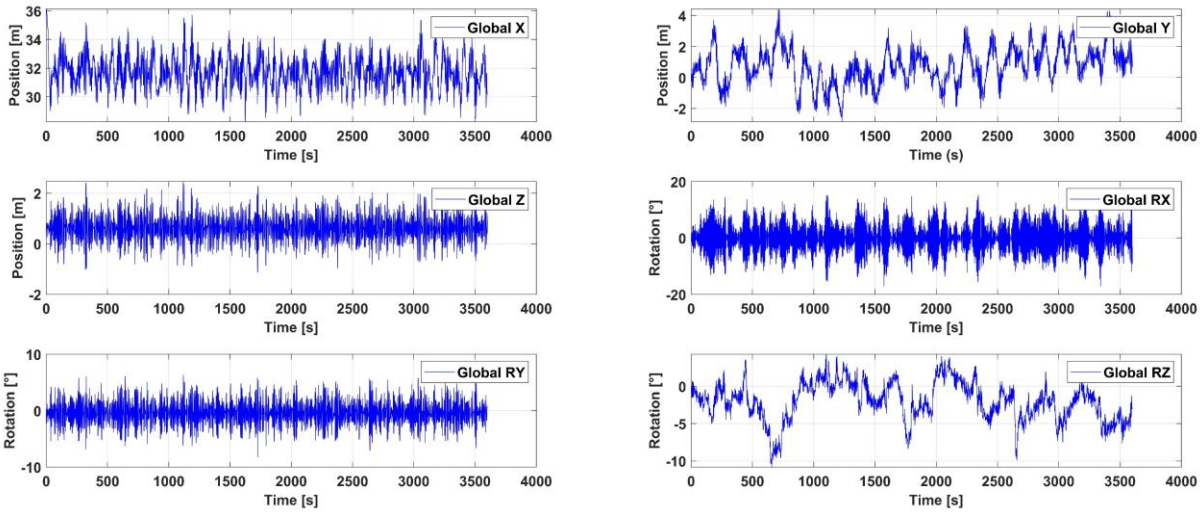

Figure 7. The structure positions of the hull in the case 1.

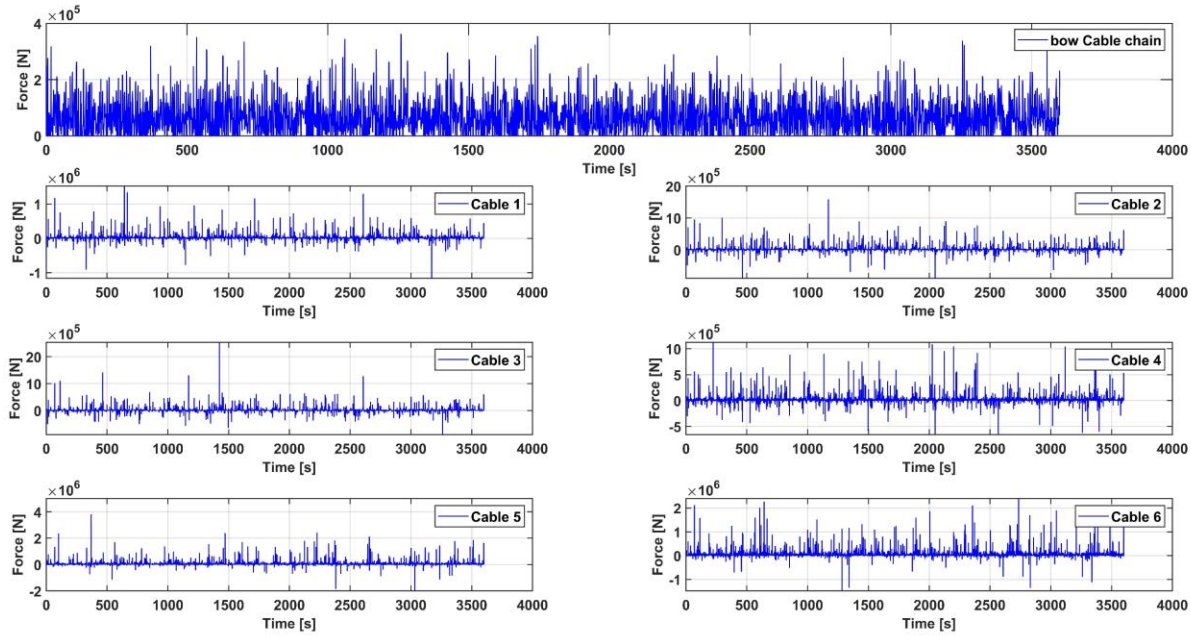

Figure 8. The tension of 7 mooring cables in the case 1.

In environmental conditions of the case 2, the structure positions of the hull in six degrees of freedom and the tension value of 7 mooring cables are shown in figure 9 and 10. The maximum tension of cables in the case 2 is 3420.2 kN in cable 6.

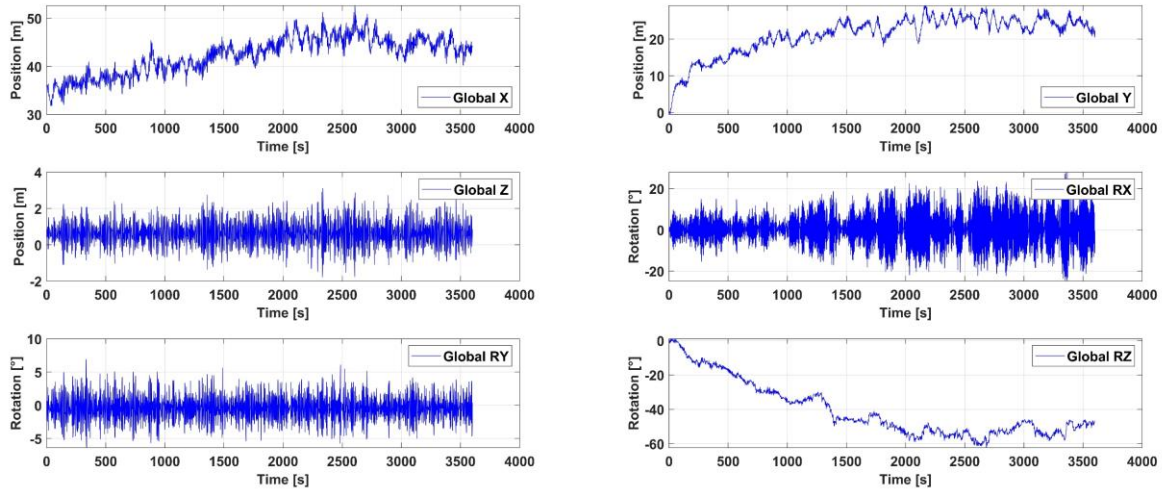

Figure 9. The structure positions of the hull in the case 2.

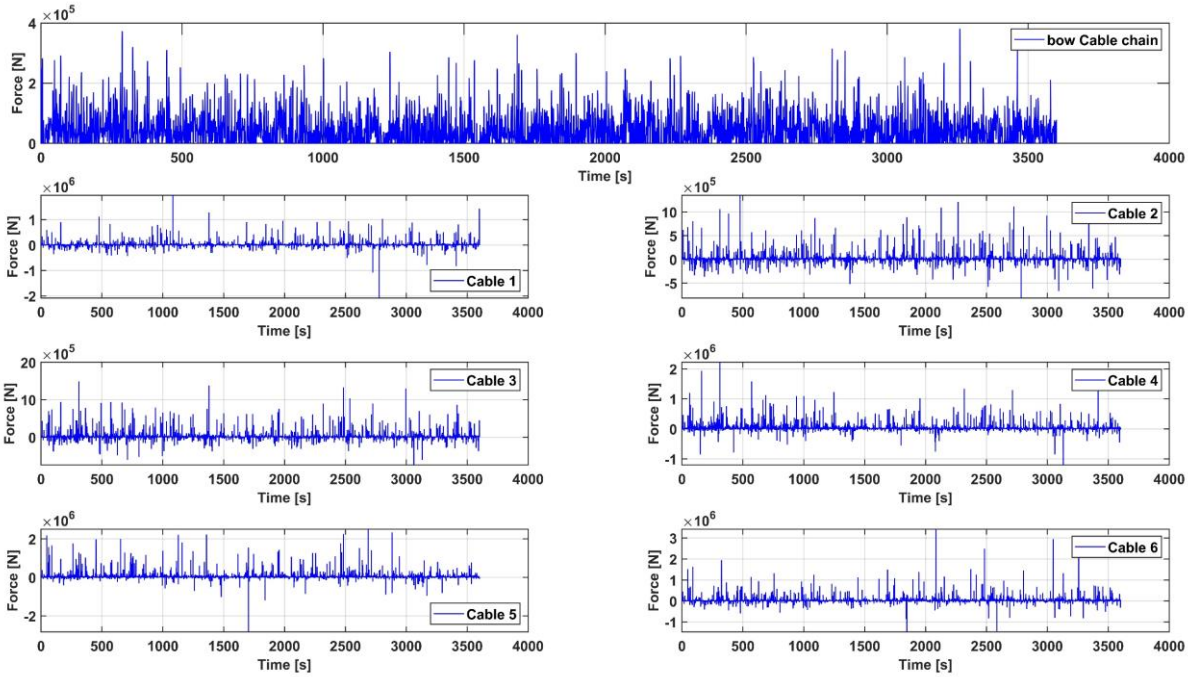

Figure 10. The tension of 7 mooring cables in the case 2.

5. Conclusion

This paper used the time-frequency domain method to calculate the structure position. The RAOs and the Froude-Krylov force have been calculated in hydrodynamic diffraction, the structure positions and the tension value of 7 mooring cables have been computed in a hydrodynamic response. The conclusions are (1) the force and moment per unit wave amplitude changed rapidly at the low-frequency domain, with frequency increasing, the force and moment stabilize gradually in general. (2) In the cross current of the case 2, the cable tensions are raised against the case 1. The security coefficient of cable tension is larger than 1.67 in two cases. And the maximum tension of two cases is smaller than the maximum tension of cables.

In this paper, the response of the tanker under the single-point mooring system is calculated and analyzed under two typical loading conditions. Practical analysis of motion response requires experiments on more environmental conditions to obtain better data for accurate predictions.

6. References

[1] ANSYS Inc 2019 *Aqwa Reference Manual*
[2] Bracco G, Giorcelli E and Mattiazzo G 2011 *Mech. Mach. Theory* **46** 1411-24
[3] Buchner B, van Dijk A and de Wilde J 2001 *Numerical Multiple-Body Simulations of Side-by-Side Mooring to an FPSO* pp 343-53
[4] Huijsmans R H M, Pinkster J A and de Wilde J 2001 *Diffraction and Radiation of Waves around Side-by-Side Moored Vessels* pp 406-12
[5] Li L, Jiang Z Y, Wang J G and Ong M C 2019 *J. Offshore Mech. Arct. Eng. Trans. Asme* **141** 9
[6] Naciri M, Waals O and de Wilde J 2007 *Time Domain Simulations of Side-by-Side Moored Vessels Lessons Learnt from a Benchmark Test* pp 801-11
[7] Pastor J and Liu Y C 2014 *J. Energ. Resour-Asme* **136**
[8] Wang K P, Ji C Y, Xue H X and Tang W Y 2017 *Ships Offshore Struc.* **12** 767-74
[9] Xu J, Liu Y and Chen C 2013 *Dynamic Response Analysis of Small Oil Tanker Based on AQWA* 779-780 pp 757-62
[10] Zhang A, Wang M, Yao M, Liu S and Wang J 2017 *Analysis of Mooring Performance Parameters of TLP Based on Aqwa* 120 pp 1369-73
[11] OCIMF 1994 *Prediction of Wind and Current Loads on VLCCs (2nd Edition)* (London: Witherby&Co. ltd) pp 3-6

Acknowledgments
This work was financially supported by grants from the Special Fund Projects for Marine Renewable Energy of the Ministry of Natural Resources of China (No. GHME2013GC01), and partial support from Natural Science Foundation of Guangdong Province of China (No. 2018A030313191, 2018A030313962) are also acknowledged.